

Optimization of Mechanical Strength Using Response Surface Methodology and Regulation of Workability in 3D-Printed Concrete with Recycled Brick Aggregate

Chenyang Liu

College of Civil Engineering, Henan Polytechnic University, Jiaozuo 454000, Henan, China

ABSTRACT

Construction-waste recycling offers a viable pathway toward sustainable concrete production. In this study, waste bricks were processed into recycled brick powder (RBP), recycled brick sand (RBS), and recycled brick coarse aggregate (RBCA) for use in single- and multi-blend 3D-printable recycled concrete, aiming to reduce natural aggregate and cement consumption. The effects of RBP, RBS, and RBCA on rheology, printability, and mechanical performance were systematically evaluated, and response surface methodology (RSM) was used to model and optimise compressive strength. Results showed that RBP had the strongest influence on rheology, increasing static and dynamic yield stresses by 50.99% and 101.61% at 30% replacement. Yield stress first increased and then decreased with increasing RBCA, reaching a peak at 20%. Rheological behaviour governed printability: higher static yield stress improved build height, whereas higher dynamic yield stress reduced extrusion width. Compressive strength showed a non-linear response, increasing by 1.26% at 10% RBP but decreasing by 24.87% and 15.33% under full RBS and RBCA replacement. RSM identified an optimal blend of 12.4% RBP, 25.1% RBS, and 51.8% RBCA, balancing sustainability and mechanical performance for 3D concrete printing.

KEYWORDS

3D-printed concrete; Recycled brick powder/aggregate; Rheological properties; Compressive strength; Response surface methodology

1. INTRODUCTION

Waste bricks account for over 30% of construction and demolition waste generated during rapid urbanisation and the renovation of historic urban areas [1]. They can be processed into recycled brick powder (RBP), recycled brick sand (RBS), and recycled brick coarse aggregate (RBCA) to replace cementitious binders and natural aggregates, thereby reducing resource consumption and the environmental burden of waste disposal [2]. Meanwhile, 3D printing concrete (3DPC) offers advantages such as reduced labour demand, lower material waste, greater design flexibility, and the elimination of formwork and vibration during construction [3]. Therefore, integrating recycled brick-based materials into 3DPC presents a promising strategy for advancing sustainable construction.

The utilisation of recycled brick materials in concrete has been widely investigated. Previous studies have shown that an appropriate amount of recycled brick powder (RBP) can improve long-term mechanical properties and durability through filler, pozzolanic, and nucleation effects, which promote a denser microstructure and continued hydration [4, 5]. For recycled aggregate concrete, mechanical and physical properties generally remain comparable to those of conventional concrete when the replacement ratio is kept within an appropriate range [6]. However, full replacement of natural aggregates may significantly reduce compressive strength and elastic modulus due to the weakened

interfacial transition zone between recycled aggregates and cement paste [7]. In contrast, partial replacement with recycled brick aggregate has been reported to improve compressive strength, flexural strength, and abrasion resistance, mainly because of its pozzolanic reactivity and micro-filling effect, although excessive replacement leads to strength deterioration [8, 9]. Similar trends have also been observed for recycled coarse aggregate, where mechanical properties remain relatively stable at low replacement levels but decrease markedly at higher substitution ratios [10, 11].

The incorporation of recycled brick materials into 3D printing concrete (3DPC) has attracted increasing attention in recent years. Due to the large specific surface area and porous structure of recycled brick powder (RBP), its incorporation generally increases water demand and significantly affects the rheological behaviour of 3DPC mixtures [12, 13]. Existing studies have shown that the mechanical performance of 3DPC is also highly dependent on RBP content, with compressive strength typically increasing first and then decreasing as the replacement ratio rises [14]. For recycled brick sand (RBS), moderate replacement can improve buildability, whereas excessive replacement may lead to a substantial increase in drying shrinkage [15]. In addition, the use of recycled brick aggregates in 3DPC has shown mixed effects on mechanical performance: some studies reported reductions in interlayer bonding and compressive strength [16], while others found improvements in strength and workability at appropriate replacement levels, although high replacement ratios may induce obvious surface defects [17].

Despite growing interest in incorporating brick-derived materials into 3D printing concrete (3DPC), their effects on overall performance remain insufficiently understood, particularly in terms of workability and mechanical properties. This study investigates the influences of replacing cement, natural sand, and coarse aggregate with recycled brick powder (RBP), recycled brick sand (RBS), and recycled brick coarse aggregate (RBCA), respectively, on the rheological behaviour, printability, and mechanical performance of 3DPC. In addition, response surface methodology (RSM) was employed to optimise the mixture design, with the aim of improving mechanical performance and promoting the efficient utilisation of recycled brick materials.

2. MATERIALS AND TEST METHODS

2.1. Materials and Mix Proportions

2.1.1. Materials

Portland cement (P·O 42.5), silica fume (SF), and recycled brick powder (RBP) were used as cementitious materials. Natural river sand, recycled brick sand (RBS), natural coarse aggregate, and recycled brick coarse aggregate (RBCA) served as aggregates. Hydroxypropyl methylcellulose (HPMC, 20 kPa·s) and a polycarboxylate superplasticizer (SP, 30% water reduction) were used as admixtures, and tap water was adopted for all mixtures.

As shown in Figure 1, waste shale bricks were crushed and sieved to obtain RBS and RBCA, while the remaining fines were ground to produce RBP. In the mix design, RBP, RBS, and RBCA partially replaced cement, natural sand, and natural coarse aggregate, respectively. The RBS had a water absorption of 16% and was graded to match natural sand (0.15–4.75 mm), while RBCA was prepared with a particle size of 4.75–10 mm to match natural coarse aggregate. The particle-size distributions of the cementitious materials are shown in Figure 2.

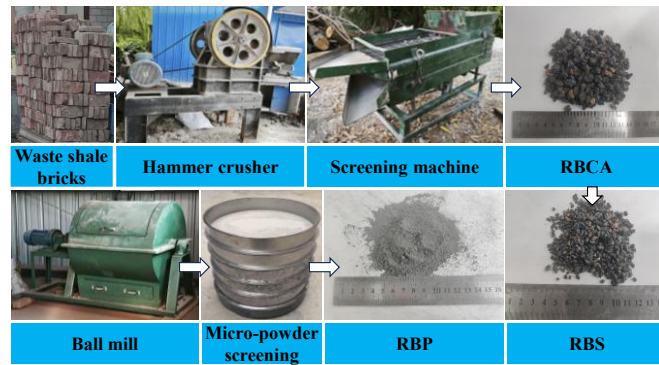


Figure 1. Preparation process of recycled brick materials

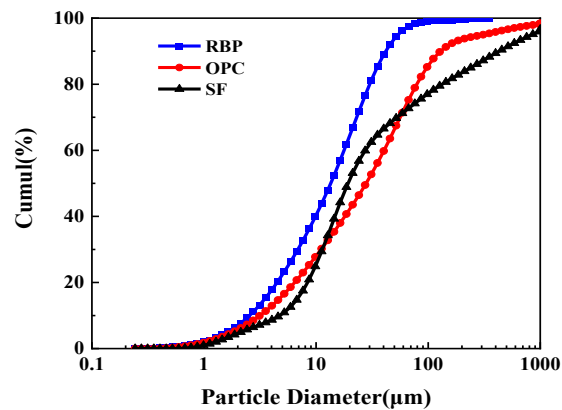


Figure 2. Particle size distribution of the cementitious materials

Table 1. Chemical Composition of Cementitious Materials (%)

Materials	SiO ₂	Al ₂ O ₃	Fe ₂ O ₃	CaO	MgO	SO ₃	P ₂ O ₅	TiO ₂	MnO
OPC	22.85	4.22	2.59	63.84	2.11	2.45	-	-	-
SF	94.77	0.09	0.57	0.16	0.32	-	-	-	-
RBP	47.87	20.70	10.77	9.31	2.23	2.27	1.00	1.16	2.23

Table 1 summarises the chemical compositions of the cementitious materials determined by XRF. The RBP mainly consists of SiO₂, Al₂O₃, Fe₂O₃, and CaO, accounting for about 93% of the total oxide content. Compared with Portland cement, RBP contains less CaO but more SiO₂ and Al₂O₃, indicating the typical characteristics of a silico-aluminous pozzolanic material and its potential as a supplementary cementitious material.

As shown in Figure 3, the XRD pattern of RBP is dominated by quartz (SiO₂) and calcite (CaCO₃), with minor amounts of dicalcium silicate (C₂S), hematite, and sodium feldspar. The quartz phase contributes to the pozzolanic reactivity of RBP [18], while calcite is beneficial to pore structure densification [19].

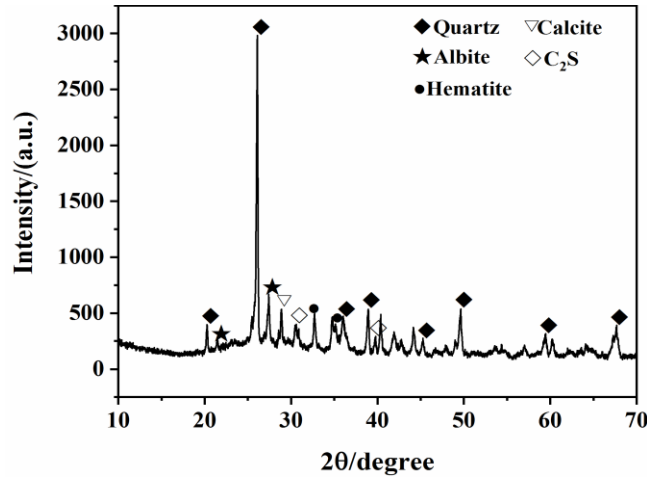


Figure 3. XRD pattern of BRP

2.1.2. Mix Proportion Design

(1) Single-factor experimental design

Ten solid-waste-based concrete mixtures containing RBP, RBS, and RBCA were designed to evaluate workability and compressive strength, and the corresponding mix proportions are listed in Table 2. Due to the high water absorption of recycled aggregates, partial replacement of natural aggregates generally reduced flowability. To compensate for this effect, RBCA was fully saturated and pre-wetted, while additional water was added to RBS according to $RBS \text{ mass} \times \text{water absorption rate} \times 70\%$. No extra water was added for RBP because of its relatively low dosage.

(2) Response Surface Optimization Experimental Design

A Box–Behnken design (BBD) was adopted to optimise the compressive strength of recycled concrete using Design-Expert 13. Compressive strength was taken as the response variable, and recycled brick powder (RBP, A), recycled brick sand (RBS, B), and recycled brick coarse aggregate (RBCA, C) were selected as the influencing factors. A three-factor, three-level response surface design with 15 experimental runs was established. The factors and coded levels are presented in Table 3.

Table 2. Single-factor mixing ratio

Specimen	OPC	SF	RBP	River sand	RBS	Stones	RBCA	W/B	SP	HPMC
G0	95%	5%	0%	100%	0%	100%	0%	0.35	1.2%	1%
P1	85%	5%	10%	100%	0%	100%	0%	0.35	1.2%	1%
P2	75%	5%	20%	100%	0%	100%	0%	0.35	1.2%	1%
P3	65%	5%	30%	100%	0%	100%	0%	0.35	1.2%	1%
S1	95%	5%	0%	80%	20%	100%	0%	0.35	1.2%	1%
S2	95%	5%	0%	40%	60%	100%	0%	0.35	1.2%	1%
S3	95%	5%	0%	0%	100%	100%	0%	0.35	1.2%	1%
A1	95%	5%	0%	100%	0%	80%	20%	0.35	1.2%	1%
A2	95%	5%	0%	100%	0%	40%	60%	0.35	1.2%	1%
A3	95%	5%	0%	100%	0%	0%	100%	0.35	1.2%	1%

Note: The proportions of binder, river sand, and coarse aggregate are 1:1:1 by mass. W/B — Water to binder ratio; G0 refers to the reference group; Groups P, S and A refer to RBP, RBS and RBCA substitution rate groups.

Table 3. Response surface experimental design

Level	Factor		
	A (RBP%)	B (RBS%)	C (RBCA%)
-1	10	20	20
0	20	60	60
1	30	100	100

2.2. Test Methods

2.2.1. Sample Preparation

Based on the 25 designed mixtures, prismatic specimens (800 mm × 120 mm × 105 mm) were printed using a Huachuang Zhizao HC1018 robotic-arm concrete 3D printer (Figure 4(b)). The printing speed and nozzle size were 25 mm/s and 40 mm × 15 mm, respectively. After printing, the specimens were covered with plastic film for 24 h and then cured at 20 ± 2 °C and relative humidity above 95%. After 28 days, they were cut into 100 mm cubes for compressive strength testing (Figure 4(d)).

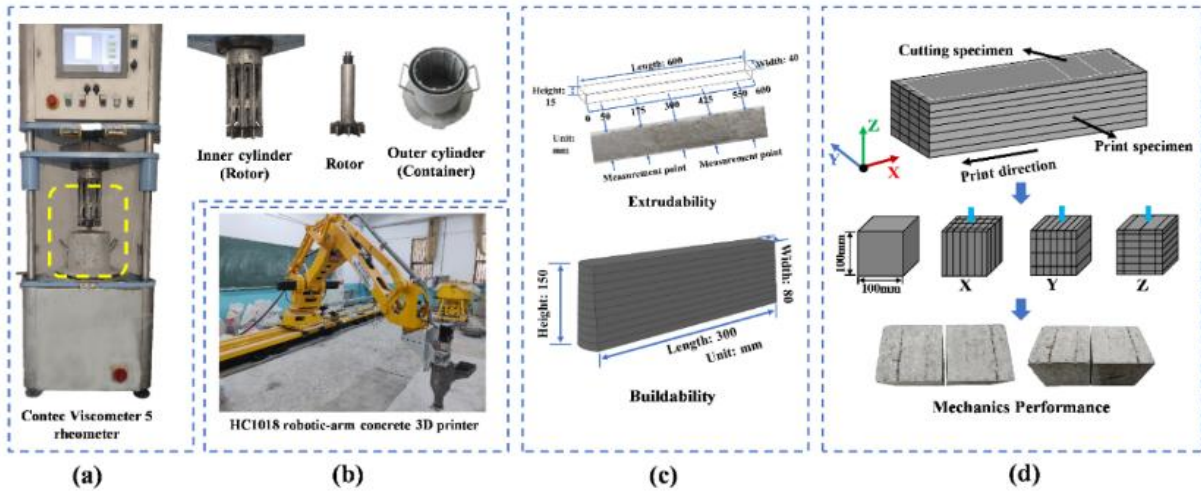


Figure 4. (a) Viscometer 5 rheometer. (b) Architectural 3D printer. (c) Extrudability and Buildability test (d) Mechanics Performance

2.2.2. Rheological Test

Yield stress was measured using a Viscometer 5 rheometer (ConTec, Iceland) (Figure 4a). The dynamic and static yield stresses were determined according to the method described in [20]. Before testing, the ten mixtures listed in Table 2 were mixed for 30 min to ensure homogeneity.

2.2.3. Printability Test

A circular nozzle with an outlet diameter of 30 mm was used to evaluate printability. For each mixture in Table 2, a 600 mm single-layer strip was printed, and the average deviation between the measured and designed widths was used to assess extrusion performance. In addition, an open specimen with a designed height of 150 mm and width of 80 mm was printed in 10 layers, and the final height variation was used to evaluate buildability.

2.2.4. Compressive Strength Test

A total of 25 mix designs were prepared, and three specimens were fabricated for each design. After casting and cutting into cubes, compressive strength was tested in the X direction according to GB/T 50081-2002. The compressive strength of each mix was taken as the average of the three specimens.

2.2.5. Box-Behnken Experimental Design Method

The BBD was adopted to improve experimental efficiency and systematically evaluate the nonlinear interactions among multiple variables. Through quadratic regression modelling, the procedure included defining the response and factor levels, generating the experimental matrix, conducting the tests, establishing and validating the regression model, and performing three-dimensional response surface analysis.

3. RESULTS AND ANALYSIS

3.1. Single-factor Test Results

3.1.1. Rheological Properties

Figure 5 shows the relationship between the rheological properties of the 3D-printed mixtures and the replacement levels of recycled brick materials. As shown in Figure 5(a), the incorporation of RBP significantly increased the static yield stress, with P1, P2, and P3 increasing by 10.65%, 26.23%, and 50.99%, respectively, compared with G0. A similar trend was observed for the RBS-modified mixtures, with static yield stress increases of 4.79%, 16.37%, and 43.54% for S1, S2, and S3, respectively. In contrast, the RBCA-modified mixtures showed a non-monotonic trend, with the static yield stress first increasing and then decreasing; the maximum increase was 6.52% in A1, whereas the reduction reached 8.25% at higher replacement levels. As shown in Figure 5(b), the dynamic yield stress exhibited a similar tendency but with greater variation. The dynamic yield stress of P3 increased by 101.61% relative to G0, while S3 reached 303 Pa, corresponding to a 73.14% increase. For RBCA, the dynamic yield stress also first increased and then decreased, with a maximum increase of 44.57% at 20% replacement.

This behaviour is mainly attributed to the material characteristics of the recycled brick constituents. The high specific surface area and water absorption of RBP reduced free water and promoted particle flocculation, thereby markedly increasing yield stress [21]. RBS also increased yield stress because its rough and porous surface enhanced interparticle friction and slurry viscosity [22]. By comparison, RBCA had a weaker effect, likely due to its lower fines content and water release during mixing [23].

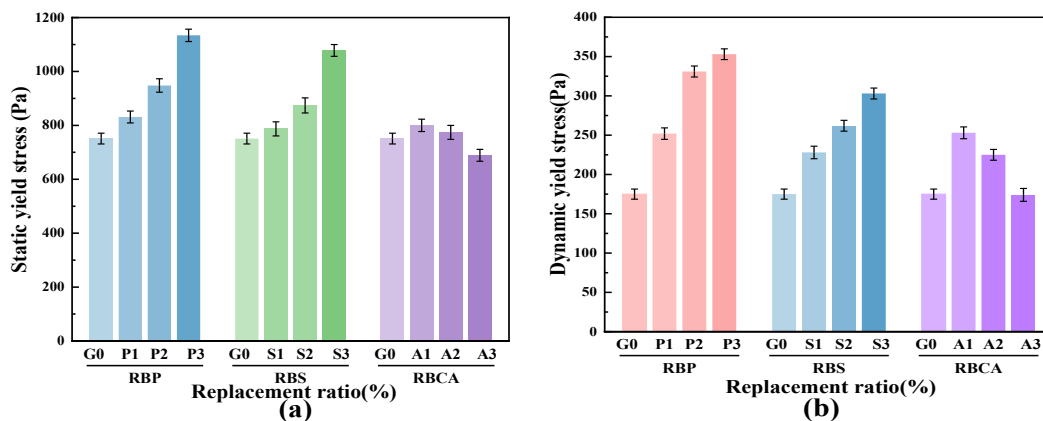


Figure 5. Relationship between yield stress and brick material replacement rate (a) Static yield stress and (b) Dynamic yield stress

3.1.2. Printability Performance

As shown in Figure 6, all mixtures containing recycled brick materials met the requirement for continuous extrusion. However, distinct differences in extrusion width and build height were observed among the replacement groups. With increasing RBP content, the extrusion width decreased by 2.14%-9.52% relative to G0, while the build height of P3 increased by 2.72% and the height deviation decreased from 3 mm to 1 mm. A similar tendency was observed for the RBS-modified

mixtures, with S3 showing a 4.52% reduction in strip width and a 2.45% increase in build height. In contrast, the RBCA-modified mixtures exhibited an opposite trend, as the extrusion width of A3 increased by 3.57% and the specimen height decreased by 0.68%. These results are in good agreement with the rheological measurements, confirming that rheological behaviour plays a dominant role in controlling extrusion quality and buildability.

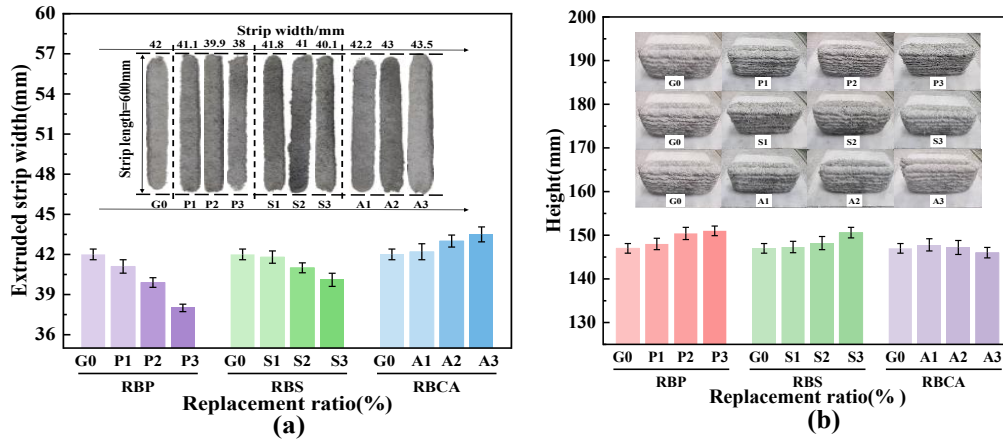


Figure 6. Relationship between Printability and brick material replacement Rate and (a) Extruded strip width (b) Wall construction height

3.1.3. Compressive Strength Analysis

Figure 7 shows the effects of different recycled brick materials on the 28-day compressive strength of 3D-printed concrete measured perpendicular to the printing direction. With increasing RBP content, the compressive strength first increased slightly and then decreased markedly. Compared with G0, specimen P1 showed a slight increase of 1.26%, whereas P3 exhibited a significant decrease of 26.38%. This indicates that an appropriate amount of RBP can improve matrix compactness and promote secondary hydration, while excessive replacement weakens strength because of insufficient cement hydration [24].

For the RBS-modified mixtures, compressive strength decreased continuously with increasing replacement ratio. The strength reduction was 4.52% at 20% replacement (S1) and reached 24.87% at 100% replacement (S3). This decline became more pronounced when the replacement ratio exceeded 20%, which was mainly attributed to the higher porosity and lower strength of RBS [25].

A similar decreasing trend was observed in the RBCA-modified mixtures. Compared with G0, the compressive strength decreased by 5.27%, 3.52%, and 15.33% at RBCA replacement levels of 20%, 60%, and 100%, respectively. The overall deterioration was mainly related to the relatively weak nature of recycled brick aggregates and the release of absorbed water from pre-wetted RBCA, which increased the effective water–binder ratio and weakened the cementitious matrix [25]. Nevertheless, the compressive strength of A2 was slightly higher than that of A1, which may be associated with the aggregate distribution and the improved aggregate–matrix compatibility at a moderate replacement level [26].

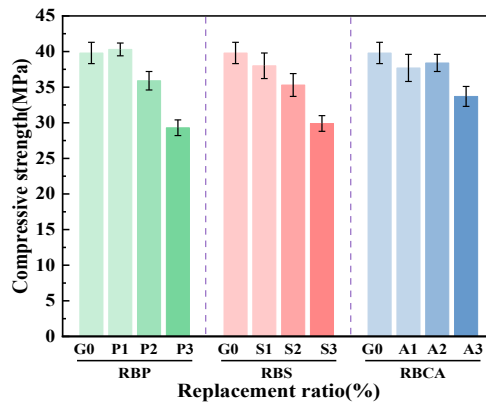


Figure 7. Relationship between compressive strength and brick material replacement rate

3.2. References Response Surface Design Optimization of Compressive Strength

3.2.1. Multi-factor Box-Behnken Experimental Design and Results

RBP, RBS, and RBCA all affect the compressive strength of recycled concrete, and their interaction effects were evident from both previous studies and the present single-factor results. To further evaluate the individual and combined influences of these three variables, the Box–Behnken design (BBD) was employed. This method enables efficient experimental design and quantitative analysis of factor contributions through regression modelling. A total of 15 runs, including 12 factorial points and 3 centre points, were conducted, and the corresponding response values are listed in Table 4. These results were used to establish the regression model and analyse the effects of RBP, RBS, and RBCA on the compressive strength of recycled concrete.

Table 4. Box-Behnken experimental design and results

Specimen	A (%)	B (%)	C (%)	Compressive strength/MPa
1	10	20	60	35.6
2	30	20	60	28
3	10	100	60	28.7
4	30	100	60	23.6
5	10	60	20	31.8
6	30	60	20	24.1
7	10	60	100	27.9
8	30	60	100	22.2
9	20	20	20	31.3
10	20	100	20	26.6
11	20	20	100	28.4
12	20	100	100	22.8
13	20	60	60	33.3
14	20	60	60	33.6
15	20	60	60	33.12

3.2.2. Mathematical Model Selection

Design-Expert 13 was used to perform analysis of variance (ANOVA) on the experimental results in order to establish an appropriate mathematical model and evaluate the interactions among key parameters. Table 5 summarises the ANOVA results.

At the 95% confidence level, a p-value below 0.05 indicates statistical significance of the BBD model. As shown in Table 5, the quadratic model was highly significant, with a sequential p-value < 0.0001.

Its lack-of-fit was not significant ($p = 0.4021$), indicating good agreement between the model and the experimental data. Moreover, the high R^2_{adj} (0.9956) and R^2 (0.9812) values confirm the strong predictive capability of the model. Therefore, the quadratic regression model was adopted for subsequent response analysis.

Table 5. ANOVA results for each model

Source	Sequential p-value	Lack of Fit p-value	Adjusted R^2	Predicted R^2	Model evaluation
Linear	0.0098	0.0055	0.5297	0.4537	
2FI	0.9693	0.0038	0.3721	0.1192	
Quadratic	<0.0001	0.4021	0.9956	0.9812	Suggested
Cubic	0.4021		0.9968		

3.2.3. Establishment of a Second-Order Regression Analysis Model

Table 6. ANOVA model for quadratic regression analysis

Source	Sum of Squares	df	Mean Square	F-value	P-value
Model	258.12	9	28.68	353.99	< 0.0001
A	85.15	1	85.15	1050.99	< 0.0001
B	58.32	1	58.32	719.82	< 0.0001
C	19.53	1	19.53	241.07	< 0.0001
AB	1.56	1	1.56	19.29	0.0071
AC	1.0000	1	1.0000	12.34	0.0170
BC	0.2025	1	0.2025	2.50	0.1747
A ²	24.39	1	24.39	301.00	< 0.0001
B ²	11.90	1	11.90	146.84	< 0.0001
C ²	67.32	1	67.32	830.92	< 0.0001
Residual	0.4051	5	0.0810		
Lack of Fit	0.2875	3	0.0958	1.63	0.4021
Pure Error	0.1176	2	0.0588		
Cor Total	258.53	14			
R ²	0.9984				
R ² _{adj}	0.9956				
Adeq Precision	57.6035				

The significance of the model terms was evaluated by analysis of variance (ANOVA), with p-values used to assess statistical significance. As shown in Table 6, the linear terms A, B, and C and the quadratic terms A², B², and C² all had p-values below 0.0001, indicating that RBP, RBS, and RBCA each had significant effects on compressive strength. The interaction terms AB and AC also showed significance ($p < 0.05$), confirming notable coupling effects between these variables. Based on the F-values, the relative influence of the three factors on compressive strength was ranked as RBP > RBS > RBCA, indicating that RBP played the dominant role.

According to the Box-Behnken design results, a quadratic regression model was established using Design-Expert 13:

$$\text{Compressive strength} = +33.34 - 3.26A - 2.7B - 1.56C + 0.625AB + 0.5AC - 0.225BC - 2.57A^2 - 1.79B^2 - 4.27C^2 \quad (1)$$

The sign and magnitude of the regression coefficients reflect the direction and degree of influence of each term on compressive strength. Positive coefficients indicate a promoting effect, whereas negative coefficients indicate an adverse effect, and larger absolute values correspond to stronger contributions.

3.2.4. Model Validation

Model validation is essential for evaluating the reliability of the regression model. As shown in Figure 8(a), the residuals are closely distributed around the red diagonal line, indicating that the model satisfies the normality assumption. In Figure 8(b), the predicted values agree well with the experimental results, further confirming the accuracy and reliability of the quadratic regression model.

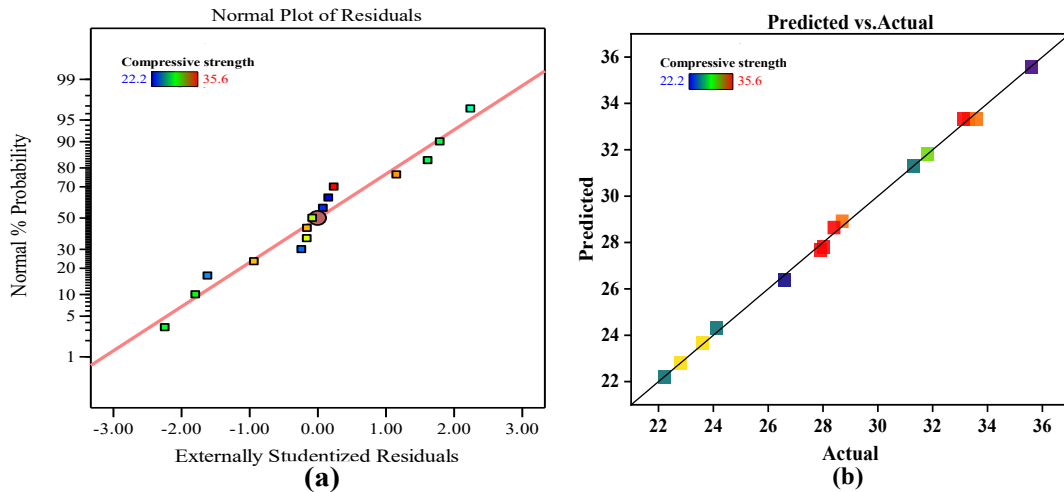


Figure 8. Response value model analysis diagram:(a) Normal plot of residuals and (b) Comparison between the actual value and the predicted value

3.2.5. Parameter Combination

In the response surface analysis, a steeper slope indicates a stronger interaction effect on compressive strength. As shown in Table 6 and Figures 9-11, the significance of the interaction terms followed the order $AB > AC > BC$, namely, $RBP + RBS > RBP + RBCA > RBS + RBCA$. Figure 9 shows that compressive strength decreased with the simultaneous increase in RBP and RBS, and the denser contours along the RBP axis indicate that RBP had a greater effect than RBS. In Figures 10 and 11, compressive strength first increased and then decreased with increasing RBCA content, with a turning point at approximately 55% replacement. The contour plots further confirm that compressive strength was more sensitive to RBP and RBS than to RBCA.

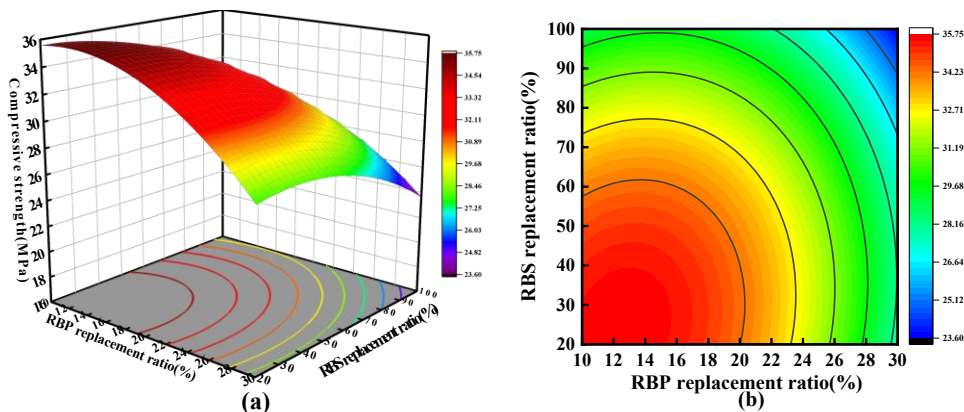


Figure 9. Response Surface and Contour Plots for the Interaction of RBP and RBS Incorporation Levels (a) Response Surface Plot (b) Contour Plot

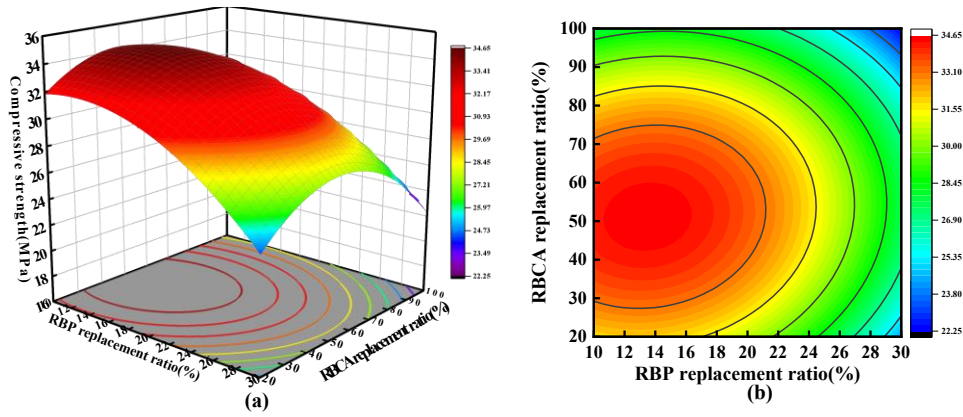


Figure 10. Response Surface and Contour Plots for the Interaction of RBP and RBCA Incorporation Levels (a) Response Surface Plot (b) Contour Plot

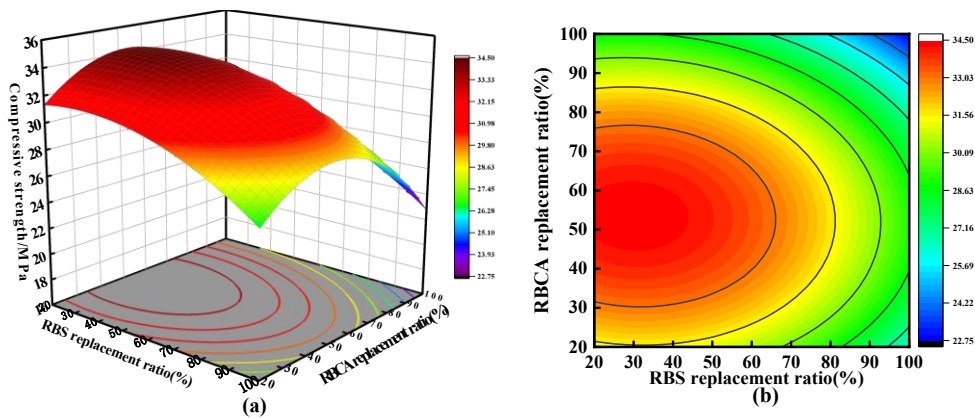


Figure 11. Response Surface and Contour Plots for the Interaction of RBS and RBCA Incorporation Levels (a) Response Surface Plot (b) Contour Plot

3.2.6. Determination and Validation of Optimal Admixture Content for Recycled Bricks with High Compressive Strength

The optimization module of Design-Expert 13 was used to determine the optimum combination of RBP, RBS, and RBCA for maximising compressive strength. The optimal mixture contained 12.397% RBP, 25.141% RBS, and 51.817% RBCA, with a predicted compressive strength of 35.973 MPa. Experimental validation yielded a 28-day compressive strength of 36.12 MPa, which agreed well with the predicted value. This result confirms the reliability and accuracy of the RSM-based optimisation model.

4. SUMMARY

RBP was used as a cement substitute, while RBS and RBCA were used to replace natural aggregates. Single-factor experiments were conducted to investigate their effects on the rheological behaviour, printability, and mechanical performance of 3DPC, and response surface methodology (RSM) was further employed to establish a predictive model for compressive strength. The main conclusions are as follows:

- (1) The incorporation of RBP and RBS significantly increased both the static and dynamic yield stresses of 3DPC, whereas saturated RBCA caused the yield stresses to first increase and then decrease. Among the three factors, RBP had the strongest influence. At 30% RBP, the dynamic and static yield stresses increased by 101.61% and 50.99%, respectively.

(2) RBP and RBS improved the buildability of the recycled concrete mixtures. Compared with G0, the filament width decreased by 9.52% in P3 and 4.52% in S3, while the height deviation was also reduced. In particular, the deviation in P3 decreased from 3 mm to 1 mm, indicating better shape retention. By contrast, the incorporation of pre-saturated RBCA reduced the achievable layer height and weakened buildability.

(3) An appropriate amount of RBP enhanced compressive strength, with a 10% replacement leading to a 1.26% increase, after which the strength gradually declined. For RBS and RBCA, the strength reductions remained limited at replacement levels of 20% and 60%, with decreases of 4.52% and 3.52%, respectively. Beyond these levels, the compressive strength deteriorated more rapidly.

(4) The combined effects of RBP, RBS, and RBCA on compressive strength were evaluated using the Box–Behnken design. The relative significance of the three factors followed the order of RBP > RBS > RBCA, and the interactions AB and AC were found to be significant. The optimal mixture proportions were 12.397% RBP, 25.141% RBS, and 51.8165% RBCA.

Overall, the conversion of waste bricks into recycled materials for partial replacement of cementitious materials and natural aggregates shows considerable environmental and engineering potential. Further studies are still needed to improve aggregate modification, enhance material compatibility, and promote the wider application of waste brick-based recycled materials in sustainable construction.

REFERENCES

- [1] Deb S, Mazumdar M, Afre R A. “Reuse of Brick Waste in the Construction Industry”, *Journal of Mines, Metals & Fuels*, Vol. 72, No. 2, 2024. <https://doi.org/10.18311/jmmf/2024/35536>
- [2] Chee Lum Wong, Kim Hung Mo, Soon Poh Yap. “Potential use of brick waste as alternate concrete-making materials: A review”, *Journal of Cleaner Production*, Vol. 195, pp. 226-239, 2018. <https://doi.org/10.1016/j.jclepro.2018.05.193>
- [3] Tu Haidong, Wei Zhenyun, Bahrami Alireza. “Recent advancements and future trends in 3D concrete printing using waste materials”, *Developments in the Built Environment*, Vol. 16, 2023. <https://doi.org/10.1016/J.DIBE.2023.100187>
- [4] Likes Lauren, Markandeya Ananya, Haider Md Mostofa. “Recycled concrete and brick powders as supplements to Portland cement for more sustainable concrete”, *Journal of Cleaner Production*, Vol. 364, 2022. <https://doi.org/10.1016/J.JCLEPRO.2022.132651>
- [5] Luo Xu, Gao Jianming, Liu Xi. “Hydration and microstructure evolution of recycled clay brick powder-cement composite cementitious materials”, *Journal of Thermal Analysis and Calorimetry*, Vol. 147, No. 20, pp. 10977-10989, 2022. <https://doi.org/10.1007/S10973-022-11343-2>
- [6] Layachi Berredjem, Nouredine Arabi, Laurent Molez. “Mechanical and durability properties of concrete based on recycled coarse and fine aggregates produced from demolished concrete”, *Construction and Building Materials*, Vol. 246, pp. 118421-118421, 2020. <https://doi.org/10.1016/j.conbuildmat.2020.118421>
- [7] Lamiaa Ismail, Mohamed Abdel Razik, El Sayed Ateya. “Optimizing sustainable concrete mixes with recycled aggregate and Portland slag cement for reducing environmental impact”, *Discover Materials*, Vol. 4, No. 1, pp. 68-68, 2024. <https://doi.org/10.1007/S43939-024-00136-Z>
- [8] Olofinnade Oluwarotimi, Ogara Joshua. “Workability, strength, and microstructure of high strength sustainable concrete incorporating recycled clay brick aggregate and calcined clay”, *Cleaner Engineering and Technology*, Vol. 3, 2021. <https://doi.org/10.1016/J.CLET.2021.100123>
- [9] L. Evangelista, J. de Brito. “Mechanical behaviour of concrete made with fine recycled concrete aggregates”, *Cement and Concrete Composites*, Vol. 29, No. 5, pp. 397-401, 2006. <https://doi.org/10.1016/j.cemconcomp.2006.12.004>
- [10] Chaocan Zheng, Cong Lou, Geng Du. “Mechanical properties of recycled concrete with demolished waste concrete aggregate and clay brick aggregate”, *Results in Physics*, Vol. 9, pp. 1317-1322, 2018. <https://doi.org/10.1016/j.rinp.2018.04.061>
- [11] Ting Wang, Shenao Cui, Xiaoyu Ren. “Study on the mechanical properties and microstructure of recycled brick aggregate concrete with waste fiber”, *Reviews on Advanced Materials Science*, Vol. 63, No. 1, 2024. <https://doi.org/10.1515/RAMS-2023-0175>

- [12] Zhiming Ma, Qin Tang, Huixia Wu. “Mechanical properties and water absorption of cement composites with various fineness and contents of waste brick powder from C&D waste”, *Cement and Concrete Composites*, Vol. 114, 2020. <https://doi.org/10.1016/j.cemconcomp.2020.103758>
- [13] Zhao Yasong, Gao Yangyunzhi, Chen Gaofeng. “Development of low-carbon materials from GGBS and clay brick powder for 3D concrete printing”, *Construction and Building Materials*, Vol. 383, 2023. <https://doi.org/10.1016/j.conbuilddmat.2023.131232>
- [14] Jiahu Shao, Jianming Gao, Yasong Zhao. “Study on the pozzolanic reaction of clay brick powder in blended cement pastes”, *Construction and Building Materials*, Vol. 213, pp. 209-215, 2019. <https://doi.org/10.1016/j.conbuilddmat.2019.03.307>
- [15] Tao Ding, Jianzhuang Xiao, Fei Qin. “Mechanical behavior of 3D printed mortar with recycled sand at early ages”, *Construction and Building Materials*, Vol. 248, pp. 118654-118654, 2020. <https://doi.org/10.1016/j.conbuilddmat.2020.118654>
- [16] Christen Heidi, van Zijl Gideon, de Villiers Wibke. “The incorporation of recycled brick aggregate in 3D printed concrete”, *Cleaner Materials*, Vol. 4, 2022. <https://doi.org/10.1016/J.CLEMA.2022.100090>
- [17] Mehdi Chougan, Szymon Skibicki, Yazeed A. Al Noaimat. “Comparative analysis of ternary blended cement with clay and engineering brick aggregate for high-performance 3D printing”, *Developments in the Built Environment*, Vol. 20, pp. 100529-100529, 2024. <https://doi.org/10.1016/J.DIBE.2024.100529>
- [18] Zhang Honglei, Cao Mingli, Xing Zhandong. “Effect of mechanical grinding time on the particle groups characteristics and activation effect of Yellow River sediment”, *Journal of Building Engineering*, Vol. 64, 2023. <https://doi.org/10.1016/J.JOBE.2022.105566>
- [19] Zeng Muling, Kim Yi-Yeoun, Anduix-Canto Clara. “Confinement generates single-crystal aragonite rods at room temperature”, *Proceedings of the National Academy of Sciences of the United States of America*, Vol. 115, No. 30, pp. 7670-7675, 2018. <https://doi.org/10.1073/pnas.1718926115>
- [20] Zhao Yu, Duan Yihang, Zhu Lingli. “Characterization of coarse aggregate morphology and its effect on rheological and mechanical properties of fresh concrete”, *Construction and Building Materials*, Vol. 286, 2021. <https://doi.org/10.1016/J.CONBUILDDMAT.2021.122940>
- [21] Luo Xu, Li Shujun, Xu Zhenhai. “Effect of recycled brick powder on the hydration process of cement paste”, *Journal of Sustainable Cement-Based Materials*, Vol. 12, No. 10, pp. 1307-1321, 2023. <https://doi.org/10.1080/21650373.2023.2216702>
- [22] He Ziming, Shen Aiqin, Wang Wenzhen. “Evaluation and optimization of various treatment methods for enhancing the properties of brick-concrete recycled coarse aggregate”, *Journal of Adhesion Science and Technology*, Vol. 36, No. 10, pp. 1060-1080, 2022. <https://doi.org/10.1080/01694243.2021.1956210>
- [23] Hou Shaodan, Duan Zhenhua, Xiao Jianzhuang. “Effect of moisture condition and brick content in recycled coarse aggregate on rheological properties of fresh concrete”, *Journal of Building Engineering*, Vol. 35, 2021. <https://doi.org/10.1016/J.JOBE.2020.102075>
- [24] Tanash Alaa Omar, Muthusamy Khairunisa, Mat Yahaya Fadzil. “Potential of recycled powder from clay brick, sanitary ware, and concrete waste as a cement substitute for concrete: An overview”, *Construction and Building Materials*, Vol. 401, 2023. <https://doi.org/10.1016/J.CONBUILDDMAT.2023.132760>
- [25] Chee Lum Wong, Kim Hung Mo, Soon Poh Yap. “Potential use of brick waste as alternate concrete-making materials: A review”, *Journal of Cleaner Production*, Vol. 195, pp. 226-239, 2018. <https://doi.org/10.1016/j.jclepro.2018.05.193>
- [26] Li Xu, Jian Wen Zhao, Gui Yun Yan. “Axial compressive behavior of recycled brick aggregate geopolymer concrete-filled corrugated tube columns”, *Journal of Constructional Steel Research*, Vol. 235, pp. 109864-109864, 2025. <https://doi.org/10.1016/J.JCSR.2025.109864>